



Enhancing tissue integration and angiogenesis of novel nanocomposite polymer using plasma surface polymerisation, an in vitro and in vivo study

| | |
|-------------------------------|---|
| Journal: | <i>Biomaterials Science</i> |
| Manuscript ID | BM-ART-07-2015-000265.R1 |
| Article Type: | Paper |
| Date Submitted by the Author: | 20-Sep-2015 |
| Complete List of Authors: | Griffin, Michelle; University College London (UCL), Division of Surgery & Interventional Science Palgrave, Robert; University College London, Department of Chemistry Seifalian, Alexander; University College London (UCL), Division of Surgery & Interventional Science Butler, Peter; Royal Free London NHS Foundation Trust Hospital, Department of Plastic and Reconstructive Surgery Kalaskar, Deepak; University College London (UCL), Division of Surgery & Interventional Sci.; Deepak Kalaskar, |
| | |

Enhancing tissue integration and angiogenesis of novel nanocomposite polymer using plasma surface polymerisation, an in vitro and in vivo study.

Michelle F. Griffin¹, Robert G Palgrave³, Alexander M. Seifalian¹, Peter E. Butler^{1, 2}, Deepak M. Kalaskar^{*1}

1. Centre for Nanotechnology & Regenerative Medicine, UCL Division of Surgery & Interventional Science, University College London, London, United Kingdom

2. Department of Plastic and Reconstructive Surgery, Royal Free London NHS Foundation Trust Hospital, London, United Kingdom

3. Department of Chemistry, University College London, 20 Gordon Street, London, WC1H 0AJ.

*Corresponding Author

Dr Deepak M kalaskar d.kalaskar@ucl.ac.uk

Centre for Nanotechnology & Regenerative Medicine,
UCL Division of Surgery & Interventional Science,
University College London, London, United Kingdom

Abstract

Current surgical reconstruction of facial defects including nose or ear involves harvesting patient's own autologous tissue, causing donor site morbidity and is limited by tissue availability. The use of alternative synthetic materials is also limited due to complications related to poor tissue integration and angiogenesis, which lead to extrusion of implants and infection. We intend to meet this clinical challenge by using a novel nanocomposite called polyhedral oligomeric silsesquioxane poly(carbonate-urea) urethane (POSS-PCU), which has already been successfully taken to the clinical bench-side as a replacement trachea, tear duct and vascular by-pass graft.

In this study, we aimed to enhance tissue integration and angiogenesis of POSS-PCU using an established surface treatment technique, plasma surface polymerisation (PSP), functionalising the surface using NH_2 and COOH chemical groups. Physical characterisation of scaffolds was achieved by using number of techniques, including water contact angle, SEM, AFM and XPS to study effect of PSM modification on POSS-PCU nanocomposite in detail, which has not been previously documented. Wettability evaluation confirmed that scaffolds become hydrophilic and AFM analysis confirmed that nano topographical alterations resulted as a consequence of PSP treatment. Chemical functionalisation was confirmed using XPS, which suggested the presence of NH_2 and COOH functional groups on the scaffolds.

The modified scaffolds were then tested both *in vitro* and *in vivo* to investigate the potential of PSP modified POSS-PCU scaffolds on tissue integration and angiogenesis. *In vitro* analysis confirmed that PSM modification resulted in higher cellular growth, proliferation and ECM production as assessed by biochemical assays and immunofluorescence. Subcutaneous implantation of modified POSS-PCU scaffolds was then carried out over 12-weeks, resulting in enhanced tissue integration and angiogenesis ($p < 0.05$).

This study demonstrates a simple and cost effective surface modification method to overcome the current challenge of implant extrusion and infection caused by poor integration and angiogenesis.

Key Words; Plasma surface modification; allyamine grafting; acrylic acid grafting; amine; carboxylic acid

1. Introduction

The cartilage framework of the nose or ear following cancer resection, trauma or congenital deformities is restored primarily by autologous tissue.¹ Autologous grafts allow surgeons to reconstruct the cartilage with a low risk of infection and extrusion as they are transferred from other sites of the patient's body, providing good biocompatibility.¹ Although autologous grafts are preferred, the donor site morbidity, limited availability has instigated surgeons to consider the use of alloplastic grafts for facial reconstruction. An alternative to using autologous grafts for nasal reconstruction is the use of alloplastic implants (synthetic materials) such as silicone.² Alloplastic grafts have many advantages including providing an unlimited supply of predetermined shapes and sizes, no donor site morbidity, reduction in operation time and complexity of surgery.² However, the currently available alloplastic grafts are limited by their infection, extrusion and migration rates, in addition to patients not being satisfied with the cosmetic look or feel.³⁻⁶ Therefore, there is an unmet clinical need to create an alloplastic graft for nose or ear reconstruction to overcome current restorative surgical techniques.

Different approaches are being investigated to prevent the extrusion of implants and improve the clinical outcome of facial implants. Evidence has shown that implants should promote tissue integration and angiogenesis to ensure anchoring of the implant to the surrounding tissue and thus the prevention of infection.⁷⁻¹⁰ To promote tissue integration of subcutaneously implants, researchers have explored modifying both the surface and bulk properties of the material.⁷ Ensuring percutaneous implants are porous will allow for tissue integration, but the mechanical properties of the scaffold must not be compromised to be able to withstand the forces *in vivo*.¹¹⁻¹⁴

Over the years, surface modification of biomaterials has been a widely accepted strategy to modify the implant interphase that first comes into contact with the body. So that, by altering surface interphase of the implant material, cell adhesion, tissue in growth and vessel formation can be supported. Plasma surface modification (PSM) is an attractive way of modifying the chemical properties of polymers without modifying the bulk properties of the material.¹⁵ PSM has been shown to modify surface chemistry, topography and affect hydrophilicity, in turn affecting protein adsorption and cell adhesion.¹⁵ Plasma surface polymerisation (PSP) is a type of PSM which lays down a desired monomer onto the surface of the polymer material, creating specific functional groups on the surface using polymerisation. Allylamine grafting has shown to functionalise the surface with amino groups and acrylic acid with carboxyl groups.¹⁶

A non-biodegradable polymer used in this study is a nanocomposite based on nano polyhedral oligomeric silsesquioxane (POSS) nanoparticle cross linked with polycarbonate-based urea-urethane (PCU, UCL-Nano™).¹⁷⁻²⁰ This polymer has been manufactured and extensively tested as various applications for synthetic organs such as the World's First Synthetic Trachea, lacrimal duct replacement and currently undergoing clinical trial as a lower limb by-pass graft. This non-

biodegradable material has been shown previously, as anti-thrombogenic²⁰, biocompatible²¹, nontoxic²² and does not cause inflammatory reactions to the surrounding host tissues.²³⁻²⁴ The presence of POSS nanocage structures in the polymer enhances the mechanical strength²⁰ whilst maintaining the radial elasticity, corrosion and oxidation resistance.²⁰ Whilst the polymer material has shown good biocompatibility and cell adhesion, the inherent hydrophobicity limited the extent of cell adhesion and potential tissue ingrowth and vessel formation.

The aim of this study was to improve the tissue integration and angiogenesis of the POSS-PCU polymer by using PSM, specifically with -NH₂ and -COOH functional groups via PSP. After functionalization the scaffolds were extensively characterised using a range of techniques, which include, water contact angle, mechanical testing, scanning electron microscopy (SEM), atomic force microscopy (AFM) and X-ray Photon Spectroscopy (XPS) to evaluate the effect of PSM on physiochemical and mechanical characteristics. Scaffolds were further investigated for *in vitro* and *in vivo* culture. The adhesion, proliferation, and collagen production of human dermal fibroblast cells (HDF) was also assessed, as they are the predominant cells in the skin, which are in contact with subcutaneous implants. Angiogenesis and tissue integration was further assessed by implanting the implants subcutaneously in a mouse model for a period of 3-months.

This study has important implications for developing new implantable materials, which promote tissue integration and angiogenesis to overcome implant failure caused by extrusion and infection, especially for developing new generation of facial implants which still remains unmet clinical challenge.

2. Materials and Methods

2.1 POSS-PCU Nanocomposite synthesis and 3D scaffold Fabrication

The polymer was synthesised, as described previously.¹⁷ In brief, polycarbonate polyol 2000 mwt was mixed with and trans-cyclohexanechloroydrinisobutylsilises-106 quioxane (Hybrid Plastics Inc) using a 500 ml flask containing a mechanical stirrer and nitrogen inlet. The POSS cage dissolves into the polyol solution using heat followed by cooling at 70⁰C. Under nitrogen at a temperature of 75-85⁰C flake 4, 4'-methylenebis (phenyl 109 isocyanate) (MDI) was then added to the mixture for a total of 90 minutes, forming a pre-polymer. To create a polymer solution dimethylacetamide (DMAC) was then added to the pre-polymer. Following cooling the 40⁰C chain extension was then carried out by the addition of ethylenediamine and diethylamine in DMAC in a drop wise manner.

The POSS-PCU polymer was fabricated as a 3D scaffold using the phase-separation (coagulation)/porogen technique NaCl was dissolved in 18% wt solution of POSS-PCU in DMAC containing Tween-20 surfactant. Stainless steel sieves were used to obtain a NaCl mixture of 200-250 μ m. The final solution was then dispersed and degassed in a Thinky AER 250 mixer (Intertomics, Kidlington, UK). A 1:1 weight ratio of NaCl to POSS-PCU was used in all experiments. The polymer mixture was then spread evenly onto circular steel moulds and directly placed into deionised water for initially 30 hours. Following this period, frequent water changes were carried out to dissolve out the NaCl porogen particles and DMAC for 7 days. As a result of both techniques 8 cm x 8 cm circular polymer sheets with 700-800 μ m thickness were synthesised. For cell culture analysis the circular sheets of polymer were cut into 16-mm diameter disks to be used in 24-well plates, using a steel manual shape cutter.

2.2 POSS-PCU 3D scaffold surface Modification with plasma

Plasma surface modification was carried out by using LF (radio frequency) plasma generator operating at 40 KHz at 100 W. Scaffolds to be treated were placed in a 24 well plate. Plasma modification was done as a 2-stage procedure, surface activation and plasma polymerisation. Surface activation was achieved by exposing scaffolds to oxygen plasma for 5 minutes, at 40 KHz with gas flow rate of 0.4 mbar. Plasma polymerisation was carried out by introducing both Allylamine (termed NH₂) and acrylic acid (termed COOH) monomers (sigma Aldrich, UK) at 0.4 mbar pressure for further 5 minutes at 100W. Scaffolds were immediately kept in a desiccator under vacuum until further use.

3.1 Characterisation of 3D scaffold

Scaffold were fully characterised using the following methodologies;

3.2 Contact Angle Measurements

The static wettability of the POSS-PCU scaffolds was analysed using sessile drop analysis. The measurements were performed using the drop-shape

analysis system DSA100 from Krüss GmbH, equipped with a CCD camera. The sessile drop was dispensed by a syringe pump through a flat tip needle of 0.5 mm diameter. A 5 µl volume of deionised water was used throughout the experiments. The captured images of sessile drops were analysed using drop-shape analysis (DSA) software (version 1.90.0.14). All measurements were performed at 20 ± 5 °C. One drop per scaffold, with 6 samples per scaffold was analysed.

3.3 Mechanical Testing

The mechanical properties of the POSS-PCU polymer was characterised using the Instron-5565 tensile 224 tester as previously described.¹⁷ Using a dog bone shaped polymer scaffold with 20 x 4 mm dimension and loading speed of 50 mm/min., the tensile properties of the scaffolds were analysed. The scaffold thickness was measured using an electronic micrometer apparatus. The Young's modulus of elasticity at 0-25% was calculated and collected for six scaffolds.

3.4 Scanning Electron Microscopy (SEM)

The surface of the POSS-PCU polymer discs was analysed using scanning electron microscope (SEM) to assess pore size and its distribution (n=3). For cell morphology analysis the discs were fixed with 2.5% w/v gluteraldehyde/PBS for 48 hours. The scaffolds were then dehydrated using a series of acetone alcohol solutions (distilled water, 50%, 70%, 90%, 100%, 100%) at room temperature and then CO₂ critically point dried. The polymer disc scaffolds were then attached to aluminium stubs with double sided sticky tabs before being coated with gold using a sc500 (EMScope) sputter coater. The polymer discs were then analysed and photographed using the FEI Quanta 200F Scanning Electron Microscope.

3.5 Porosity Measurements

The porosity of the scaffolds (n = 3) was analysed as previously described using the following formulas¹⁷:

Firstly, the thickness and the overall precise dimensions of the porous POSS-PCU implants were calculated, enabling the volume of the scaffold to be documented. The POSS-PCU scaffolds were then weighed. The scaffold mass was then divided by the scaffold volume to calculate the overall apparent density of the polymer as per equation 1.

Equation 1:

$$\text{Apparent Density (g/cm}^3\text{)} = \frac{\text{Scaffold mass (g)}}{\text{Scaffold volume (cm}^3\text{)}}$$

This value was then divided by the overall apparent density of the POSS-PCU ($\rho = 1.15$ g/cm³). The porosity was then expressed as a percentage as per equation 2.

Equation 2:

$$\text{Porosity (\%)} = \left(\frac{1 - \text{scaffold density (g/cm}^3\text{)}}{\text{POSS - PCU polymer density (g/cm}^3\text{)}} \right) \times 100\%$$

3.6 X-ray photoelectron spectroscopy (XPS) studies

The surface composition and chemistry of the modified scaffolds were characterised using a Thermo Scientific K-alpha spectrometer (Department of Chemistry, UCL, UK). Monochromatic Al K α X-rays ($h\nu = 1486.6$ eV) were focused to a 400 μm diameter spot on the scaffold surface, defining the analysis area. The analysis depth at this photon energies 5-10 nm. Survey spectra were conducted to determine the elemental composition of the surface. High-resolution spectra of the principle core line of each element present were then acquired for chemical state identification. Where necessary, these high resolution spectra were fitted with Gaussian-Lorentzian peaks using CasaXPS software to deconvolute different chemical environments.

3.7 Atomic Force Microscopy (AFM)

The POSS-PCU surface topography was examined using an atomic force microscope (TAP150A) operating in tapping mode using a spring constant 2.919 n/m. The root mean square roughness (RSM) was calculated from the 5 μm scan of three areas using the NanoScope $^{\text{®}}$ analysis software (Bruker Corporation) version 1.40. Using Nanoscope $^{\text{®}}$ analysis the PeakForce quantitative nanomechanical mapping was calculated to obtain a FV modulus using the modified Hertzian model. Three areas of the 5 μm scan were analysed for their mechanical properties.

3.8 BCA protein Assay

Total serum protein adsorption on unmodified and modified samples was determined by BCA assay as described previously.²⁵ Briefly scaffolds were incubated with complete growth medium at 37 $^{\circ}\text{C}$ for 24 hours. The medium was removed before transferring the scaffolds to another 24 well plate. The scaffolds were washed three times with PBS before adding BCA reagent to each well and leaving for incubation at 37 $^{\circ}\text{C}$. The absorbance was then measured at 562 nm. Scaffolds incubated in serum free medium were used as a control (n=6).

4 Biocompatibility of POSS-PCU Plasma Surface Modification

Human dermal fibroblast (HDF) adhesion and proliferation was tested as a measure of biocompatibility of the POSS-PCU modified scaffolds.

4.1 Cell Culture and Cell Seeding

Human Dermal fibroblasts (HDFs) primary cells obtained from the European Collection of Cell Culture (ECACC) were cultured in Dulbecco's Modified Eagle's medium (DMEM) supplemented with 10% Fetal Bovine Serum (FBS) and 1% antibiotic solutions (all from Sigma, UK). For cell culture experiments the 16 mm polymer disks were sterilized using 70% ethanol and washed three times with sterile phosphate buffer solution (PBS) and placed into the 24 well plates, before cell seeding. Each polymer disk was seeded with 1×10^4 cells /cm². Media was changed every two days.

4.2 Cellular adhesion and morphology

To study cell adhesion and morphology of the fibroblasts on the POSS-PCU scaffolds, immune-cytochemistry staining was carried out. First the media was removed from the 24-wells and then the cells were washed with PBS three times. Following this the cells were fixed with 4% (w/v) paraformaldehyde in PBS pre warmed at 37⁰C and left for 10-15 minutes. Cells were then washed with 0.1% tween 20 thrice, followed by addition of 0.1% tritonX100 to improve permeability and left for 5 minutes. Then Rhodamine Phalloidin dye, was added in the ratio 1:40 (diluted in 1000 μ l of methanol) in PBS and left for 40 minutes. Cells were then washed three times and then mounted onto slides with DAPI to stain the nuclei. The cells were then mounted and then visualized under fluorescence microscopy (n=6).

4.3 Metabolic activity of cells

To assess the cytotoxicity and viability, the commercially available assay Alamar blueTM (Life Technologies, UK) was used. Scaffolds were put in 24 well plates and sterilized as explained before. After cells were seeded for specific time point, prior to assay, scaffolds were moved to fresh well plates to only account for cell seeded on the scaffolds. Alamar blue assay was then performed as per manufacturer's instructions. Briefly, after 4 hours of incubation with Alamar blue dye, 100 μ l of media was place into 96 well plates and fluorescence was measured at excitation and emission wavelength of 530 and 620 nm using Fluoroskan Ascent FL, (Thermo Labsystems, UK). As this assay is non-toxic to cells, same set of scaffolds were used for further testing by washing them with PBS and replacing with fresh cell culture media (n=6).

4.4 Cell proliferation using DNA Quantification

To assess fibroblast cells proliferation a Fluorescence Hoechst DNA Quantification Kit was utilized to quantify the DNA content on the POSS-PCU scaffolds (Sigma, UK). Assay was performed as per manufacturer's instructions The fluorescence was measured with excitation set at 360 nm and emission at 460 nm using Fluoroskan Ascent FL, (Thermo Labsystems, UK) (n=6).

4.5 Collagen production

Collagen production was confirmed by using 2 assays, namely Picro Sirius red and hydroxyproline quantification.

A] The extracellular collagen production by the fibroblasts was analysed at day 7 and 14 using the Picro Sirius Red (PSR) method as per manufacturer's instruction. Dye contains a reagent that specifically binds to collagen. Briefly, cells were first fixed in methanol overnight at -20 °C. After washing with PBS they were staining at room temperature for 4 hours with the PSR stain (0.1%) (Sigma Aldrich, UK).²⁶ Excess dye was washed with PBS three times and 0.1% acetic acid.²⁶ The stained cells were then dried for spectrophotometric analysis. The PSR solution was eluted in 200 µl of 0.1N sodium hydroxide per well. The solution was placed on a rocker at room temperature for 1 hour before the optical density (OD) was calculated at 540 nm with the Anthos 2020 micro plate reader (Biochrome Ltd, UK). A reference standard was formulated using 1, 5, 10, 20, 30, 40 and 50 µg of bovine collagen dissolved in deionized water was constructed prior to analysis of the polymer scaffolds (n=6).

B] Hydroxyproline content at 7 and 14 days were measured using a QuickZyme hydroxyproline assay according to manufacturing instructions (n=6).

4.6 Histological Analysis for in vitro scaffolds

The migration of cultured fibroblasts within the scaffolds was determined using histology. Following a 14-day culture, the polymer constructs were harvested and fixed with 4% paraformaldehyde for 24 hour at 4 °C. Following dehydration through a series of graded ethanol solutions, the solutions were paraffin embedded and horizontally cross sectioned (2-4 µm) from the middle area and analysed with Haematoxylin and Eosin (H&E) staining (n=3).

4.7 In vivo analysis

After plasma modification the 16 mm discs were subcutaneously implanted in 4-month-old BALB/c mice (Charles River Laboratories, UK) with body weight of 200g (n=4). First, the mice were anesthetized with Isoflurane and the incision site was marked with clorhexane. A small incision was made followed by implantation of the scaffold disc. The incision was then closed with 5-0 Monocryl (Ethicon, Somerville, NJ) mattress sutures. All animals were monitored on a daily basis. No adverse events were noted with any of the animals. During the experiments, the animals were housed in groups and had free access to water and pellet food. All experiments were approved by the local governmental animal care committee and were conducted in accordance with the UK legislation on the protection of animal and the guidelines for the care and Use of Laboratory Animals.

4.8 Histology and Immunohistochemistry following in vivo studies

After 12 weeks the animals were sacrificed by CO₂ asphyxiation and the scaffolds were explanted, fixed in 4% paraformaldehyde and analysed for tissue integration and angiogenesis. Scaffolds preparations were embedded in paraffin and then (3 µm) sections were cut and stained with H&E and Massons Trichrome according to standard procedures. In addition, scaffolds were stained against CD31 to detect endothelial cells. The sections were then imaged using a digital slide scanner NanoZoomer-XT C12000, Hamamatsu Photonics. To

quantify the extent of cellular integration onto the scaffold, 5 fields of view (40x magnification) were chosen at random and the percentage of tissue infiltrated in view was divided by the tissue stained by H&E staining to formulate a percentage. To quantify vessel formation, methodology was used as per previous study.²⁷ Briefly, the capillary number was calculated by identifying a positive endothelial cell cluster with a morphologically identifiable vessel with a lumen in 5 fields of view at 40x magnification on each scaffold, providing 20 fields of view in total.

5 Statistical Analysis

Statistical analysis of the results was performed using Graph Pad (Prism). Statistical significance was calculated by two-way and one-way ANOVA, with Tukey HSD post-hoc analysis where $P < 0.05$ value was considered statistically significant.

6. Results

6.1 Characterisation of scaffolds

1.1 Water Contact Angle (WCA)

Wettability is determined by measuring water contact angle (WCA) before and after PSP of POSS-PCU scaffolds. Figure 1A shows typical images of WCAs obtained following respective surface modification. From measurements it is clear that wettability of unmodified POSS-PCU scaffolds decreased significantly ($p < 0.05$) from $89 \pm 3^\circ$ to $12 \pm 2^\circ$ and $54 \pm 5^\circ$ following PSP using NH_2 and COOH respectively. This results thus confirm that wettability is altered following PSP of POSS-PCU scaffolds, this is useful parameter, which is strongly co-related with cell-interfacial interactions.^{28,29}

6.2 Mechanical Properties

6.2.1 Bulk Mechanical properties

The bulk mechanical properties of the scaffolds were assessed using an Instron-5565 tensile 224 tester. There were no differences between unmodified and COOH and NH_2 scaffolds in their mechanical properties including the maximum tensile strength, elongation at break and young's elastic modulus (Figure 1B). This confirms that PSP did not affect the bulk mechanical properties of POSS-PCU.

6.2.2 Micro Mechanical properties

The surface elastic modulus was tested after PSP to the POSS-PCU scaffolds. AFM was used to assess the surface micromechanical properties, which demonstrated that after PSM the surface elastic modulus of POSS-PCU (Figure 1C) significantly increased ($p < 0.01$). There was no significant difference between $-\text{NH}_2$ and $-\text{COOH}$ treated scaffolds ($p = 0.52$). This confirms that PSP modification of POSS-PCU increases surface micro-mechanical properties,

which is an important as this property is known to have effect on cell-interfacial interactions of biomaterials.³⁰

6.3 Surface roughness using AFM

The surface roughness is an important parameter which known to have an effect on cell behaviour.³¹ This why roughness of scaffolds was measured both pre and post PSP. Scaffolds used in this study are porous and it is difficult to access roughness of porous surfaces. However, based on SEM analysis is it clear that scaffolds have flat interfaces where AFM measurement was feasible. Care was taken to scan 3 random areas per scaffolds and mean RMS roughness was reported. Figure 1D, shows that RMS roughness of unmodified POSS-PCU scaffold increased significantly post PSP ($p < 0.05$). There was however no significant difference in the roughness between NH_2 or COOH modifications ($p < 0.55$). After plasma modification of scaffolds with NH_2 and COOH groups, no effect was observed on the pore structure of the scaffolds, with 200-250 μm pore size evident by SEM for all scaffolds (Figure 2).

6.4 Surface Analysis using X-ray Photon Spectroscopy (XPS)

Surface chemistry of PSP modified scaffolds was characterised using XPS. The surface elemental composition after plasma polymerisation using XPS is shown in Figure 3 and Table 1. The composition of the unmodified POSS-PCU surface is similar to that reported previously³², and is broadly consistent with the empirical formula. In the unmodified POSS-PCU a single, narrow symmetric N1s peak was detected at a binding energy of 399.8 eV, corresponding well to nitrogen in amide or amine groups (Figure 3).³³ The C1s region showed a strong peak corresponding to a graphitic or aliphatic carbon, with a shoulder at higher binding energy in the region expected for carbon bound to oxygen or nitrogen, again consistent with the expected structure. The O1s region shows a principle peak at 532.0 eV, with a smaller shoulder at higher binding energy. These two environments may correspond to oxygen in carboxyl groups and bound to Si.

Upon plasma treatment with either amine or carboxyl, the concentration of Si fell relative to the other elements. This suggests that the POSS-PCU is being coated, leading to the Si signal being attenuated by the material deposited during the plasma treatment. The C1s, N1s and O1s peaks all became significantly broader and asymmetric after plasma treatment, indicating a range of chemical environments present. Notably, the C1s and N1s peaks showed additional environments at higher binding energy compared with the unmodified POSS-PCU scaffold, indicating more highly oxidised groups. The peaks from these environments are not resolved due to their similar binding energies. Such peak shapes cannot be reliably fitted to any particular model so precise identification of the chemical environments present or their concentrations is not possible. However, the nitrogen content on the surface NH_2 was higher than POSS-PCU. Similarly the oxygen content was higher on the COOH than POSS-PCU. Additionally, the NH_2 scaffolds showed broader N1s and O1s peaks with components at higher binding energy, corresponding to more oxidised nitrogen and carbon environments. Therefore the two different plasma treatments lead to significantly different surface chemistry.

7 In vitro Assessment of 3D scaffolds

7.1 Protein Adsorption

Protein adsorption is important for cell attachment and growth. The total serum protein adsorption was evaluated on the PSM scaffolds and unmodified scaffolds using the BCA assay. Protein adsorption was significantly higher ($p < 0.01$) on PSM scaffolds than unmodified scaffolds as shown in Figure 5E at 24 hours. There was no significant difference in the protein adsorption between COOH and NH₂ modified scaffolds.

7.2 Cellular attachment and morphology

Anchorage dependant cells need to attach to the surface in order to proliferate and function normally. Figure 4 shows F-actin staining of HDF cells on both unmodified and modified POSS-PCU scaffolds after 24 hours of seeding. Actin organisation and stress fibre formation is essential for cell attachment, migration and proliferation. All scaffolds irrespective of surface showed polygonal and spread morphology. The mean cell area and circularity was used as a measure to quantify these differences using Image J analysis software (figure 4), which demonstrated no difference between HDF morphology on scaffolds after PSP.

7.3 Cellular activity and proliferation

To evaluate effect of PSM modification of POSS-PCU scaffolds, both metabolic activity and cell proliferation was determined over a period of 14 days using Alamar blue and DNA assay. HDFs showed similar behaviour in terms of their metabolic activity and proliferation when seeded on these scaffolds as shown in Figure 5. Significantly higher number of HDFs attached to PSP modified scaffolds compared to unmodified POSS-PCU within 24 hours of seeding (as shown in Figure 5 A and B, and a similar trend continued over the period of the experiment, suggesting enhanced cell attachment metabolic activity and proliferation on PSP modified scaffolds. Tissue culture plastic (TCP) was used as positive control; on which cell growth was significantly higher ($p < 0.01$) compared to all test scaffolds. However, within NH₂ and COOH modification, differences in cell proliferation become more pronounced after 7 days post seeding ($p < 0.01$).

7.4 Cellular In growth

Since the scaffolds used in this study were porous, migration of cells within 3D scaffolds was determined using SEM and histological analysis. SEM was used to compare cellular confluence on top of the scaffolds, which was supported with histological analysis. H&E staining from the middle section of scaffolds, suggest that after two-weeks of culture the fibroblasts migrated to the centre of the scaffolds, secreting a thin extracellular matrix into and around the pores (Figure 6A-F). A greater number of cells migrated and invaded the scaffold in NH₂

compared to COOH than unmodified POSS-PCU scaffolds by the end of the 14-day period (Figure 6G-I).

7.5 Collagen Production

Extracellular matrix (ECM) production is an important function of anchorage dependent cells. Cells produce various types of proteins and proteoglycans in their native state. One of most common ECM proteins is collagen, which is predominantly produced by growing HDFs. Here, collagen produced by cells was compared between scaffolds, which can be used as a marker of cellular function. Collagen production was evaluated by measuring collagen content indirectly using PSR staining and hydroxyproline methods (as shown in Figure 7). Collagen production was significantly higher ($p < 0.01$) on NH_2 and COOH groups compared to unmodified POSS-PCU and TCP at day 7. A similar trend existed at day 14 with collagen production doubled on all scaffolds, with the highest production on NH_2 and COOH scaffolds ($p < 0.01$) (Figure 7). Low values of collagen on TCP are likely to be because of its 2D structure compared to 3D scaffolds used in this study. However, no difference in collagen production was observed between NH_2 and COOH groups.

7.6 In vivo assessment of scaffolds - Assessment of tissue integration and angiogenesis *in vivo*

In order to verify *in vitro* results and effectiveness of plasma modification for tissue integration and evaluate potential of this treatment to enhance angiogenesis *in vivo* study was undertaken for a period of 12 weeks in a mice model. Figure 8 shows histology and immunohistochemistry of explanted unmodified and plasma modified scaffolds. The effectiveness of plasma modification was compared with unmodified control. Tissue ingrowth was confirmed using H&E staining, which showed after 12 weeks ingrowth was significantly greater in the NH_2 and COOH scaffold than unmodified scaffolds (figure 8A, NH_2 $61.45 \pm 9.8\%$, COOH $57.65 \pm 9.1\%$ and POSS-PCU $34.45 \pm 4.7\%$). There was no difference in cellular in growth between COOH and NH_2 after 12 weeks. Similarly, Masson Trichrome showed greater positive collagen staining after 12 weeks for NH_2 and COOH than unmodified scaffolds (Figure 8B). In addition, vascularisation of the scaffold after 12 weeks was significantly greater for the NH_2 and COOH scaffolds compared to POSS-PCU scaffolds as shown by the significantly higher number of identifiable capillaries (NH_2 $8.35 \pm 1\%$, COOH $8.3 \pm 1.2\%$ and POSS-PCU $3.4 \pm 0.8\%$) (Figure 9).

Discussion

The nanocomposite material POSS-PCU investigated in this study, has been shown previously to be non-toxic and a good biomaterial candidate for translational medicine in experimental and first in man studies.²¹⁻²⁴ Whilst the nanocomposite material has shown good biocompatibility, the inherent hydrophobicity (water contact angle of $89 \pm 3^\circ$) limits the extent of cell adhesion and potential tissue ingrowth and vessel formation.

This study aimed to investigate the effect of PSP on POSS-PCU scaffolds with NH_2 and COOH groups and their effect on tissue integration and angiogenesis. PSP is well established, simple and efficient way of functionalising biomaterials surfaces. Using NH_2 and COOH functional modification of materials with PSP is by far the most common method of surface modification to improve cell adhesion and proliferation. There are only limited studies *in vivo* analysis³⁴⁻³⁶ of these functional groups and thus their long term effect on tissue integration and angiogenesis still remains unclear. This study aims to fill this gap in the research.

Physiochemical characterisation of POSS-PCU scaffolds showed significant changes to its surface properties after introduction of NH_2 and COOH functional groups via PSP treatment. A significant effect on the water contact angle, surface roughness and surface chemistry was observed after PSP of POSS-PCU scaffolds. Plasma surface modification is known to have an effect on various surface properties, which include wettability and surface roughness.³⁷⁻³⁹ However, it does not affect bulk properties, which is clear from bulk mechanical analysis (Figure 1B) and structural analysis by SEM (Figure 2). However, when micro mechanical properties at surface were investigated by nano indentation using AFM, significant increase in surface mechanical properties was observed after PSM modification. Interestingly both NH_2 and COOH modification resulted in similar values of micro mechanical properties (NH_2 404 ± 82 MPa and COOH 359 ± 125 MPa) and roughness (NH_2 221 ± 21 nm and COOH 174 ± 33 nm).

Chemical modification of POSS-PCU was confirmed using XPS analysis and changes in water contact angle. Presence of C, N and O along with Si was used to identify POSS-PCU background spectra, where part of O and Si signal is related to POSS nanocage and part of C, N and O is from the PCU component.³² The XPS analysis of the NH_2 and COOH modified surfaces showed a significant difference between the scaffolds surface chemistry (Figure 3). In both cases, attenuation of the Si signal from the underlying POSS-PCU indicated deposition of material during the plasma treatment process. The XPS probing depth is around 10 nm, meaning that if a continuous film were formed films of this thickness or more would be expected to totally attenuate the Si signal from the substrate. The presence of a reduced intensity Si signal indicates deposition of <10 nm thickness of material. For both surface treatments, the carbon content was also reduced. This is likely due to removal of surface carbon contamination by the plasma process, or that the newly deposited surface is less carbon rich than POSS PCU. Due to reduction of both C and Si content, the absolute percentage of N and O increased in both COOH and NH_2 modified surfaces. However, the NH_2 modified surface was more nitrogen rich, with a N: O ratio of 0.16 compared 0.10 in the COOH modified surface. In addition to XPS, water contact angle values showed a significant change from $89 \pm 3^\circ$ for unmodified samples to $12 \pm 2^\circ$ for NH_2 and $54 \pm 5^\circ$ for COOH modified samples. From these results we can suggest that even though surface roughness remained same for both COOH and NH_2 modification, a unique change in WCA was due to the presence of individual chemical functional groups. Taken as a whole, these results are consistent with successful NH_2 and COOH surface modification of POSS PCU.

After confirming successful plasma surface functionalisation of POSS-PCU scaffolds, *in vitro* cell culture studies were performed. Early cellular response to these modified scaffolds was investigated by looking at their cell morphology and their attachment within 24 hours. Interestingly, cells on both unmodified and modified samples showed no significant difference in their morphology or spreading as quantified by the average cell area and circularity. However, when analysing cell attachment, a significantly higher number of cells attached to NH₂ ($p < 0.01$) and COOH ($p < 0.001$) scaffolds compared to unmodified samples.

Cell attachment and spreading is closely linked with the presence of cell adhesion proteins on biomaterial surfaces. When provided in the right concentration and conformation, anchorage dependant cells attach to protein binding sites via focal adhesion formation, which help cells in their migration and also decides their spreading and actin cytoskeleton organisation. Fibroblast cell spreading is usually associated with the adsorption of appropriate concentration and conformation of protein on the biomaterial surface from serum containing media.²⁹ To investigate if protein adsorption is responsible for enhancing cell attachment on the modified scaffolds, total adsorbed protein quantification was undertaken. From Figure 5E, it is clear that higher protein was adsorbed on NH₂ and COOH scaffolds compared to unmodified samples. It is hypothesised that although there was low protein adsorption on unmodified POSS-PCU, the adsorption of the protein existed in a conformation, which promoted cell spreading similarly to the modified samples. However, low amount of adsorbed protein meant that available protein was non-uniformly distributed on unmodified scaffolds, leading to low cell attachment. However, when the surface was modified with functional groups via PSP, more protein became available due to resultant higher adsorption (as seen from Figure 5E), leading uniform distribution of protein in appropriate conformation to induce both higher cell attachment and cell spreading. A schematic diagram showing this hypothesis is presented in Figure 10.

Protein adsorption from blood protein happens within a few seconds of its contact with the biomaterial surface. However, the concentration and conformation depends on various physio-chemical and mechanical properties of the material. Incremental amount of evidence suggest that chemistry^{16, 29, 40} topography^{16, 29, 41-42} and micro-mechanical properties^{16, 43} have a significant effect on protein adsorption and its conformation.⁴⁴

In this study, PSP modification results into both higher roughness and micro mechanical properties compared to unmodified POSS-PCU scaffolds. This suggests that combination of these properties have a significant effect on changes in morphology and cell attachment seen in this study. The early effect of increased cell attachment on modified scaffolds leads to significantly higher cell growth as shown by DNA and Alamar blue assay in long term culture as shown in Figure 5 C and D.

One of advantages of using plasma polymerisation technique is it uses carrier gases to modify samples and thus provide a greater ability to access pores in 3D structures.⁴⁵ The proof of which can be gathered from histological analysis post cell seeding, where cell ingrowth on PSM modified scaffolds is higher than

on unmodified scaffolds (as shown in Figure 6). To complement this qualitative assessment of cell in growth, extracellular matrix production *in vitro* was studied by the quantification of collagen produced by cells on these scaffolds. An increase in the collagen production by HDFs over the 14-day period was observed on the NH₂ and COOH scaffolds. This increase was significantly higher compared to unmodified POSS-PCU ($p < 0.01$). Previous study, has found that collagen production per cell (total DNA) can be affected by modifications in nanoscale dimensions.⁴⁶ Furthermore, fibroblast collagen production has shown to be enhanced on hydrophilic surfaces, which was observed after PSM modification of POSS-PCU. The decreased collagen production on TCP is likely due to its 2D structure compared to 3D POSS-PCU scaffolds.⁴⁷⁻⁴⁸

In addition, to *in vitro* experiments, *in vivo* studies were performed to understand the effect of tissue integration and angiogenesis. Figure 8 shows representative images of scaffold implanted for 12 weeks. No foreign body reactions were observed after modification with PSM to POSS-PCU. Histological analysis using H&E confirmed that after subcutaneous implantation plasma modified POSS-PCU scaffolds allowed for tissue migration at differing rates (Figure 8A). Masson Trichrome confirmed that a collagen production was significantly greater after modification compared to unmodified scaffolds (Figure 8B). Following PSM the surrounding tissue integrated to a greater extent after 12 weeks as shown by H&E staining. To date only few studies have documented the effect of plasma modification *in vivo*.³⁴⁻³⁶ Recently published work by Valence *et al*³⁵ looked at *in vivo* effect of air plasma modification biodegradable vascular grafts and showed enhance vascularisation for their polycaprolactone scaffold. However, there are only two relevant studies published recently looked at effect of amine and carboxyl functional modification of polymers *in vivo*.^{34, 36} Cheng *et al* tested the effect of plasma treatment modified electrospun fibres with amine groups and showed increased cell infiltration.³⁶ Whereas, Qi and colleagues³⁴ studied the effect of amine groups post plasma polymerisation on stainless steel implants and showed that implants coated with amine group showed improved tissue compatibility *in vivo* experiments. To the best of author's knowledge, there is no published work comparing effect of both amine and carboxyl groups *in vivo*, illustrating the importance of this work. PSP modification of POSS-PCU scaffold showed significantly increased endothelial migration and neovascularisation compared to unmodified POSS-PCU scaffold (Figure 9). Staining the scaffolds for CD31 illustrated a greater extent of angiogenesis in the POSS-PCU scaffolds modified with PSM. Based on the results it is clear that PSP modification of POSS-PCU can enhance ingrowth and angiogenesis, however there was no significant difference observed between NH₂ and COOH functionalisation (Figure 9).

Since results from this study showed that plasma modification is a useful technique for enhance tissue integration and angiogenesis. For applications such as ear reconstruction, another important consideration for successful integration is the mechanical properties of the materials. Matching the elastic modulus of the polymer to that of the native auricular tissue has been suggested to be an approach to prevent extrusion of implant materials used auricular reconstruction.¹⁷ A previous study by our group found the stiffness of human

auricular cartilage to be around 5 MPa.¹⁷ Our polymer demonstrated to have an elastic modulus of around 0.6-0.7 MPa, which is similar to auricular cartilage, unlike currently use Medpor implants that have a stiffness in the region of 141 MPa.¹⁷ It is clear from this study, that the plasma surface treatment does not affect the bulk properties and can be used to enhance tissue integration and angiogenesis simultaneously.

Using PSM to improve the biocompatibility of POSS-PCU for facial organs such as the ear is a highly clinically translatable technique due to the ease, simplicity and low costs of the modification. Since the scaffold treatment was carried out on the same day for both *in vitro* and *in vivo* experiments, long term stability of PSP modified scaffolds in storage was not investigated in the current study. However, knowing that hydrophobic recovery of polymer post plasma modification is reported previously⁴⁹, it will be relevant future work, which will be taken into consideration.

Conclusion

Plasma surface polymerisation (PSP) was used to modify the physiochemical properties of POSS-PCU scaffolds. It is demonstrated that scaffolds modified by PSP can significantly increase fibroblast adhesion, proliferation and collagen production via *in vitro* analysis. Followed by *in vivo* analysis, PSM has shown to enhance tissue integration and angiogenesis. This study has implications for the development of simple, cost effective method of surface functionalisation of biomaterials where enhanced tissue integration and angiogenesis is highly desired.

Acknowledgements

The Medical Research Council (MRC) and Action Medical Research (AMR) (GN2239) funded this study.

Author Contributions

All authors have reviewed the data and approved of the final manuscript.

Competing Financial Interests

None

References

1. A Sajjadian, R Rbinestein and N Naghshineh, *JPRAS*, 2010, **125**, 40.
2. A Sajjadian, R Rbinestein, N Naghshineh, *JPRAS*, 2010, **125**, 99.
3. MS Godin, SR Waldman and CM Jr Johnson, *Arch Otolaryngol Head Neck Surg*, 1995, **121**, 1131-1136.

4. I Niechajev, *Aesthet Plast Surg*, 1999, **23**, 395-402.
5. RW Kridel, *Facial Plast Surg Clin North A*, 1995, **3**, 473-486.
6. RJ Konior, *Arch Otolaryngol Head Neck Surg*, 1992, **118**, 1188-1194.
7. BD Ratner *et al.* Biomaterials Science; An introduction to materials in medicine. 3rd edn. Academic Press 2012.
8. JL Frodel, S Lee. *Arch Otolaryngol Head Neck Surg*, 1998, **124**, 1219-1223.
9. A Uysal *et al*, *J Craniofac Surg*, 2006, **17**, 1129-36.
10. DA Dickerson *et al*, *J Orthop Surg Res*, 2013, **8**, 18.
11. S Tarafder *et al*, *Biomed Mater Res B Appl Biomater*, 2015, 103, 679-90.
12. WS Sheidan, GP Duffy, BP Murphy, *J Mech Behav Biomed Mater*, 2012, **8**, 58-70.
13. T Lou *et al*, *Int J Biol Macromol*, 2014, **69**, 464-70.
14. H Kim *et al*, *Mater Sci Eng C Mater Biol Appl*, 2014, 40, 324-35.
15. B Gupta *et al*, *Biomaterials*, 2002, **23**, 863-871.
16. MS Sheu, DM Hudson and IH Loh, Biomaterial surface modification using plasma gas discharge processes. In: Wise, DL.; Trantolo, DJ.; Altobelli, DE.; Yaszemski, MJ.; Gresser, JD.; Schwartz, ER., editors. Encyclopedic handbook of biomaterials and bioengineering, Part A: Materials. Marcel Dekker, New York: 1995. p. 865-894.
17. L Nayyer, M Birchall, AM Seifalian, G Jell, *Nanomedicine*, 2014, **10**, 235-46.
18. P Jungebluth *et al*, *Lancet*. 2011, **378**, 1997-2004.
19. K Chaloupka, M Motwani, AM Seifalian, *Biotechnol Appl Biochem*, 2011, **58**, 363-70.
20. AM Seifalian, S Handcock, HJ Salacinski, and Polymer for use in conduits and medical devices? Patent Number: WO2005070998: 2005.
21. RY Kannan *et al*, *Cell Biochem Biophys*, 2006, **45**, 129-136.
22. G Punshon *et al*, *Biomaterials*, 2005, **26**, 6271-6279.
23. BX F *et al*, *Polymer* 2003, **44**, 1499-1506.
24. TS Haddad and JD Lichtenhan, *Macromolecules*, 1996, **29**, 7302-7304.
25. D Sankar *et al*, *Tissue Eng Part A*, 2014, **20**, 1689-702.
26. BJ Walsh *et al*, *Anal Biochem*, 1992, **203**:187-9.
27. T Fonseca-Silva *et al*, *Int Endod*, 2012, **45**, 859-64.
28. RE Rawsterne *et al*, Ulijn, *Acta Biomater*, 2007, **3**, 715-721.

29. DM Kalaskar *et al*, Merry, SJ Eichhorn, *Soft Matter*, 2008, **4**, 1059-1065.
30. Y Yang *et al*, *ACS Nano*, 2012, **23**, 8591-8.
31. A Scislowska-Czarnecka *et al*, *J Biomed Mater Res A*, 2015, May 26 .
32. Tan A *et al*, *Biointerphases*, 2013, **8**, 23.
33. RJJ Jansen, H Van Bekkum, *Carbon*, 1995, **33**, 1021-1027.
34. P Qi *et al*, *ACS Biomater, Sci. Eng*, 2015, June 10.
35. SD Valence *et al*, *Eur J Pharm Biopharm*, 2013, **85**, 78-86.
36. Q Cheng *et al*, *Tissue Eng Part A*, 2013, **19**, 1188-98.
37. L Ying *et al*, *Biomacromolecules*, 2003, **4**, 157-65.
38. H Rebl *et al*, *Acta Biomater*, 2012, **8**, 3840-51.
39. SH Keshel *et al*, *Int J Nanomedicine*, 2011, **6**, 641–647.
40. Y Arima Y and H Iwata, *J. Mater. Chem*, 2007, **17**, 4079-4087.
41. RC Ball, M Blunt, and W Barford, *Journal of Physics A: Mathematical and General* 1989, **22**, 2587.
42. K Rechendorff K *et al*, *Langmuir*, 2006, **22**, 10885-8.
43. RJ Delahaije RJ *et al*, *Colloids Surf B Biointerfaces*, 2014,**123**, 199-20
44. Mena *et al*, *Biomaterials*, 2008, **29**, 2710-8.
45. M Domingos *et al*, *Acta Biomater*, 2013, **9**, 5997-6005.
46. Padmanabhan J *et al*, *ACS Nano*. 2014, **18**, 4366-75.
47. Abbott A, *Nature*, 2003, **424**, 870-2.
48. Wang F *et al*, *Proc Natl Acad Sci U S A*, 1998, **5**, 14821-6.
49. P Alves *et al*, *Colloids Surf B Biointerfaces*, 2014, **113**, 25-32.

Figure Headings

Figure 1 Characterisation of the nanocomposite scaffolds after Plasma Surface Modification. [A]. Water contact angle measurements (n=6). [B]. Bulk mechanical properties (n=6). [C] Surface mechanical properties (n=3). [D] Surface nano topographical roughness analysis (n=3). Where, NH₂ is POSS-PCU scaffold modified with allylamine grafting, COOH is POSS-PCU scaffold modified with acrylic acid, and POSS-PCU is Unmodified scaffolds.

Figure 2. [A] Structure of nanocomposite polymer using scanning electron microscopy (SEM) surface (A-C) and transverse views (D-F) (n=3). Where, NH₂ is POSS-PCU scaffold modified with allylamine grafting, COOH is POSS-PCU scaffold modified with acrylic acid, and POSS-PCU is Unmodified scaffolds.

Figure 3. [A] X-ray photoelectron spectroscopy (XPS) spectrum of the nanocomposite POSS-PCU films after plasma surface modification. [B] Table illustrating the elemental composition of the nanocomposite POSS-PCU scaffolds after plasma surface modification. Where, NH₂ is POSS-PCU scaffold modified with allylamine grafting, COOH is POSS-PCU scaffold modified with acrylic acid, and POSS-PCU is Unmodified scaffolds.

Figure 4. [A] Cell morphology staining of the human dermal fibroblasts (HDFs) after 24 hours on POSS-PCU scaffolds treated with plasma surface modification. By 24 hours HDFs were well adhered and spread on the nanocomposite scaffolds. [B] Cell area analysis at 24 hours showed no difference in HDF cell morphology on POSS-PCU after 24 hours after plasma surface modification. [C] Cell circularity analysis at 24 hours showed no difference in HDF cell morphology on POSS-PCU after 24 hours after plasma surface modification. Where, NH₂ is POSS-PCU scaffold modified with allylamine grafting, COOH is POSS-PCU scaffold modified with acrylic acid, and POSS-PCU is Unmodified scaffolds. Red: Actin Blue: DAPI (n=6).

Figure 5 [A] Cell viability of human dermal fibroblasts (HDFs) on the scaffold measured using Alamar blue assay. NH₂ and COOH showed a significantly higher cell viability compared to POSS-PCU but not tissue culture plate (TCP) at 24 hours ($p < 0.05$). [B] DNA content significantly increased of the HDFs after 24 hours on NH₂ compared to COOH and POSS-PCU ($p < 0.05$). [C] NH₂ showed a significantly higher cell viability compared to POSS-PCU-COOH and control POSS-PCU but not tissue culture plate (TCP) at 3 to 14 days ($p < 0.05$) [D] DNA content significantly increased of the HDFs after 14 days on NH₂ compared to COOH and POSS-PCU from 3 to 14 days ($p < 0.05$). Where, NH₂ is POSS-PCU scaffold modified with allylamine grafting, COOH is POSS-PCU scaffold modified with acrylic acid, and POSS-PCU is Unmodified scaffolds (n=6). [E] Protein adsorption was increased after NH₂ and COOH modification compared to unmodified scaffolds at 24 hours (n=6) ($p < 0.01$).

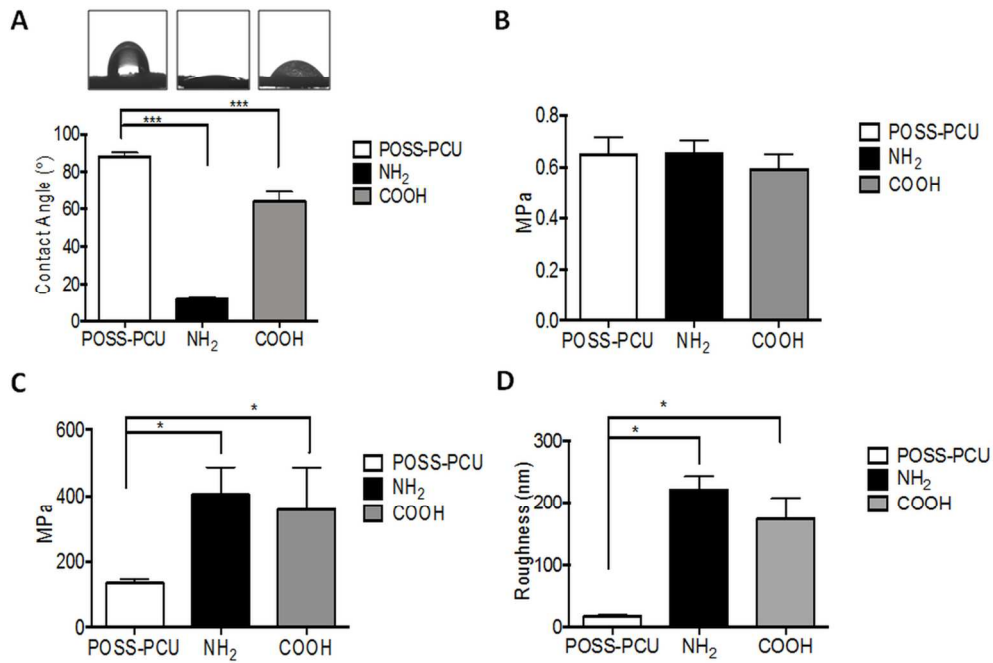
Figure 6. [A] Scanning electron microscopy images of the HDF cells at 14 days, showing cells are laying down a thin extracellular matrix at 14 days on all nanocomposite scaffolds (A-F). [B] Histology using H&E staining taken from the middle of the scaffolds (G-I). Where, NH₂ is POSS-PCU scaffold modified with allylamine grafting, COOH is POSS-PCU scaffold modified with acrylic acid, and control is Unmodified POSS-PCU (n=6).

Figure 7. Collagen production produced by human dermal fibroblasts (HDFs) [A] Collagen detected in the supernatant was assessed using Picrosirius Red staining. HDFs seeded on NH₂ showed greater collagen production at 14 days compared to all nanocomposite surfaces including tissue culture plate ($p < 0.05$). [B] Hydroxyproline content was higher by cells seeded on NH₂ and COOH than POSS-PCU ($p < 0.05$). Where, NH₂ is POSS-PCU scaffold modified with allylamine grafting, COOH is POSS-PCU scaffold modified with acrylic acid, and POSS-PCU is Unmodified scaffolds (n=6).

Figure 8. Subcutaneous implantation of POSS-PCU scaffolds after modification with PSM for 12 weeks. [A] Tissue integration assessed by H&E Staining. Collagen production was assessed by Masson Trichome. [B] Quantification of cellular integration and growth after 12 weeks. Where, NH₂ is POSS-PCU scaffold modified with allylamine grafting, COOH is POSS-PCU scaffold modified with acrylic acid, and control is Unmodified POSS-PCU.

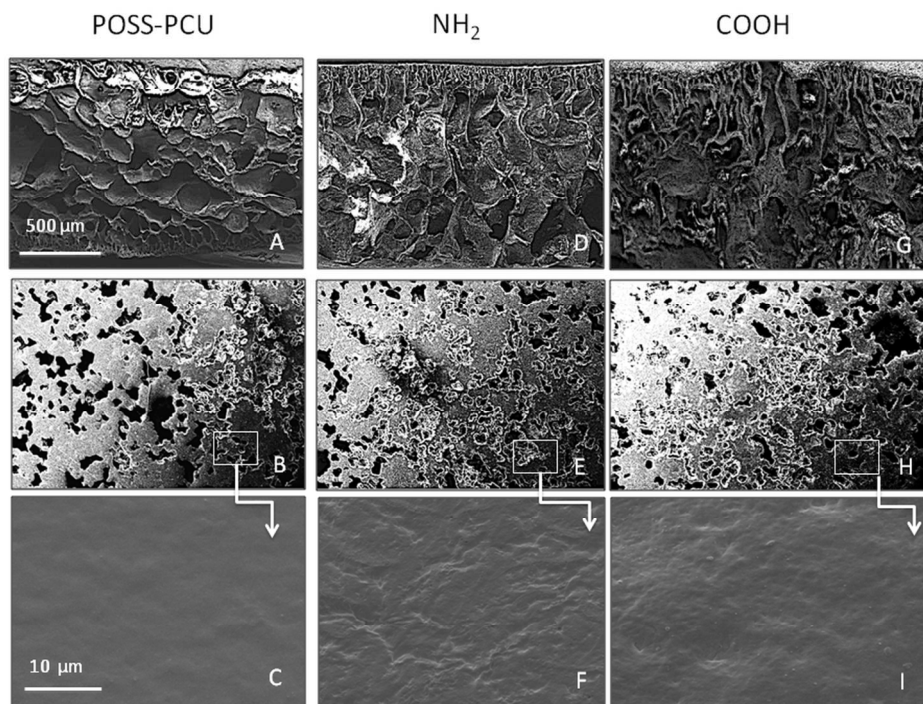
Figure 9. [A] Endothelial cell infiltration as identified by CD31 staining, which was used as a marker of angiogenesis. [B] Quantification of capillary infiltration into the scaffolds after 12 weeks. Where, NH₂ is POSS-PCU scaffold modified with allylamine grafting, COOH is POSS-PCU scaffold modified with acrylic acid, and POSS-PCU is Unmodified scaffolds (n=6).

Figure 10. Schematic representation of fibroblast cell attachment to the plasma modified and unmodified scaffolds. The roughness increased on the plasma modified scaffolds, enhance total protein adsorption thus allowing enhance fibroblast attachment of cells at 24 hours.



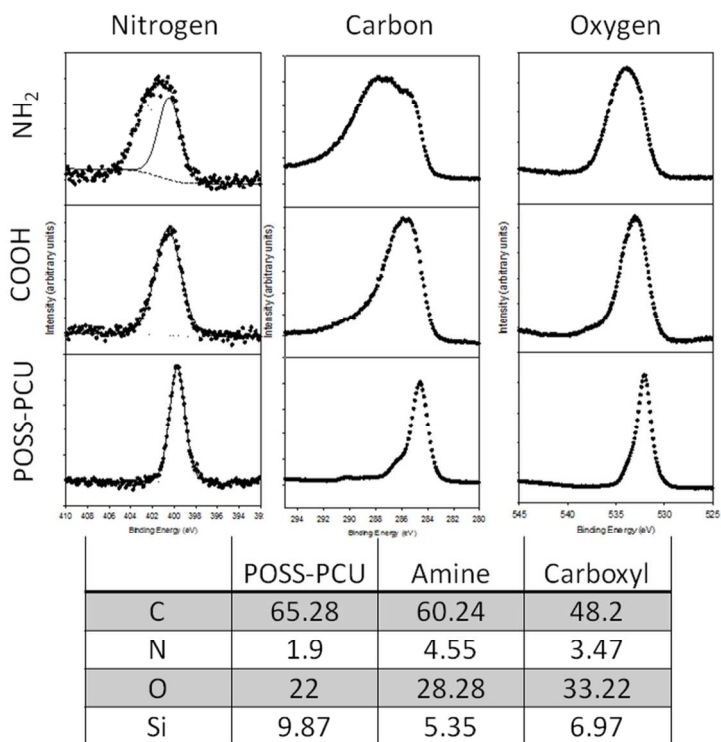
Characterisation of the nanocomposite scaffolds after Plasma Surface Modification. [A]. Water contact angle measurements (n=6). [B]. Bulk mechanical properties (n=6). [C] Surface mechanical properties (n=3). [D] Surface nano topographical roughness analysis (n=3). Where, NH₂ is POSS-PCU scaffold modified with allylamine grafting, COOH is POSS-PCU scaffold modified with acrylic acid, and POSS-PCU is Unmodified scaffolds.

127x95mm (300 x 300 DPI)

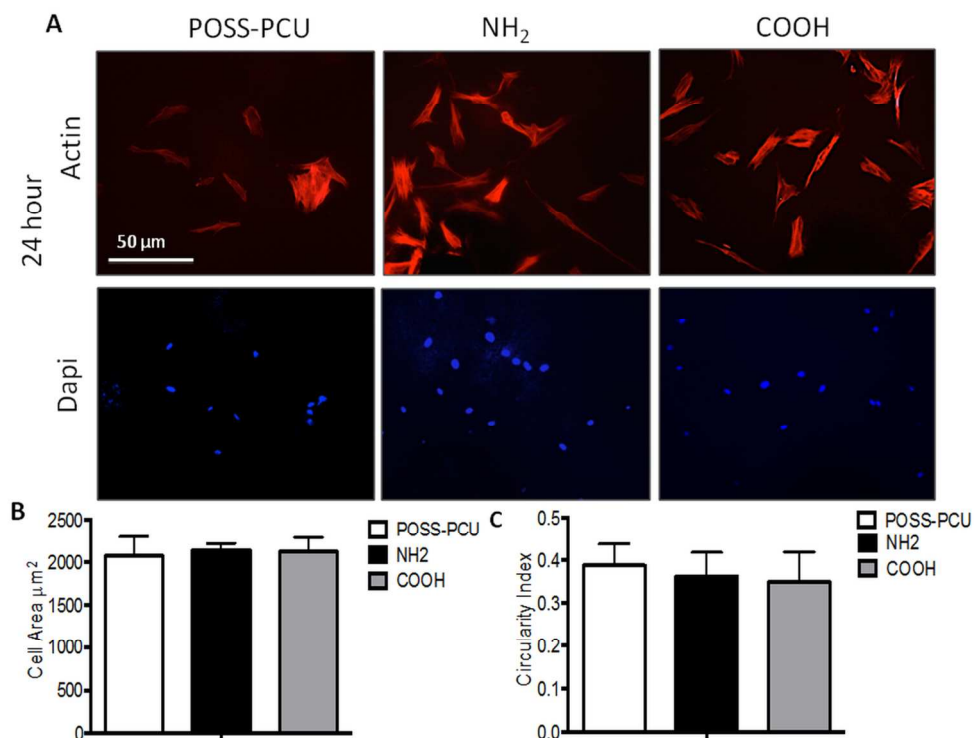


[A] Structure of nanocomposite polymer using scanning electron microscopy (SEM) surface (A-C) and transverse views (D-F) (n=3). Where, NH₂ is POSS-PCU scaffold modified with allylamine grafting, COOH is POSS-PCU scaffold modified with acrylic acid, and POSS-PCU is Unmodified scaffolds.

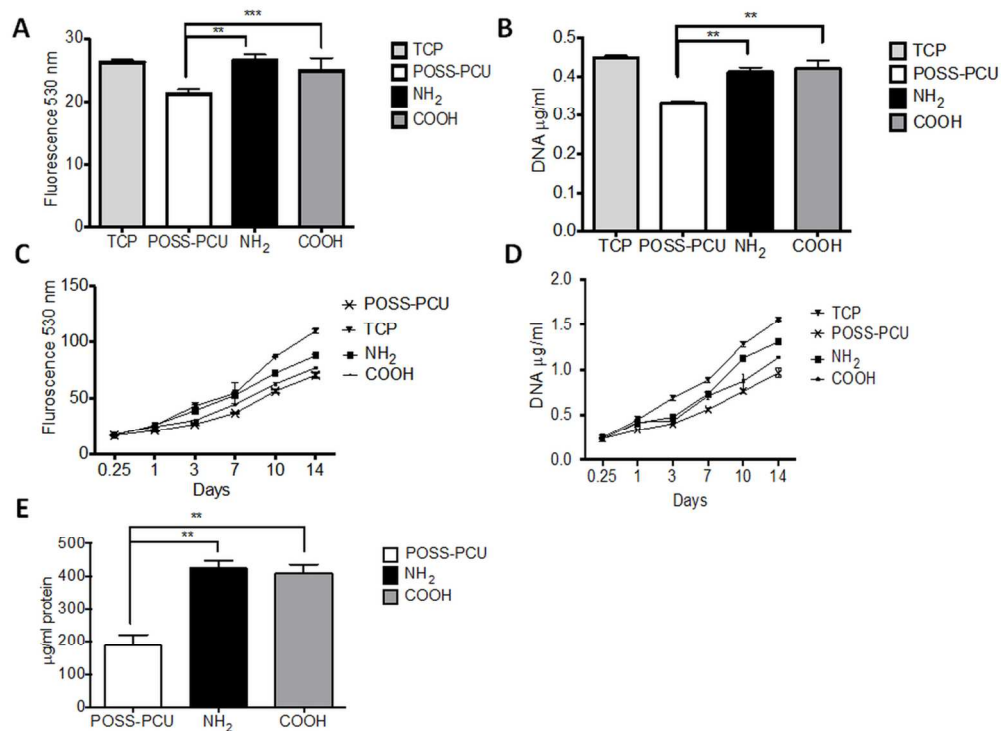
127x95mm (300 x 300 DPI)



[A] X-ray photoelectron spectroscopy (XPS) spectrum of the nanocomposite POSS-PCU films after plasma surface modification. [B] Table illustrating the elemental composition of the nanocomposite POSS-PCU scaffolds after plasma surface modification. Where, NH₂ is POSS-PCU scaffold modified with allylamine grafting, COOH is POSS-PCU scaffold modified with acrylic acid, and POSS-PCU is Unmodified scaffolds. 127x95mm (300 x 300 DPI)

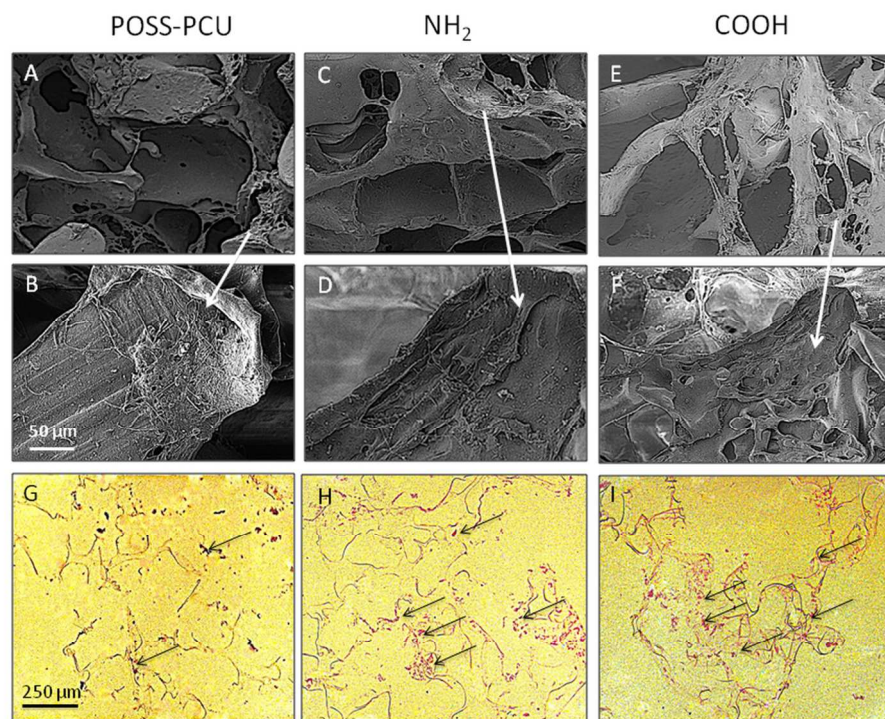


[A] Cell morphology staining of the human dermal fibroblasts (HDFs) after 24 hours on POSS-PCU scaffolds treated with plasma surface modification. By 24 hours HDFs were well adhered and spread on the nanocomposite scaffolds. [B] Cell area analysis at 24 hours showed no difference in HDF cell morphology on POSS-PCU after 24 hours after plasma surface modification. [C] Cell circularity analysis at 24 hours showed no difference in HDF cell morphology on POSS-PCU after 24 hours after plasma surface modification. Where, NH₂ is POSS-PCU scaffold modified with allylamine grafting, COOH is POSS-PCU scaffold modified with acrylic acid, and POSS-PCU is Unmodified scaffolds. Red: Actin Blue: DAPI (n=6).
127x95mm (300 x 300 DPI)

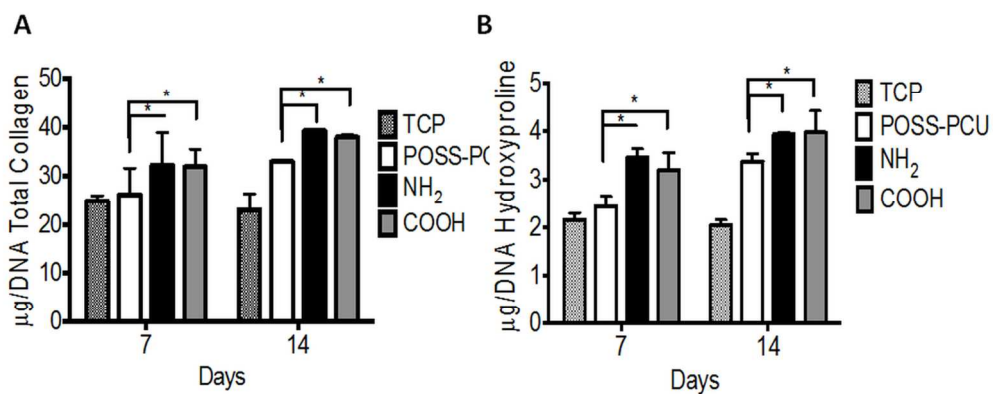


[A] Cell viability of human dermal fibroblasts (HDFs) on the scaffold measured using Alamar blue assay. NH₂ and COOH showed a significantly higher cell viability compared to POSS-PCU but not tissue culture plate (TCP) at 24 hours ($p < 0.05$). [B] DNA content significantly increased of the HDFs after 24 hours on NH₂ compared to COOH and POSS-PCU ($p < 0.05$). [C] NH₂ showed a significantly higher cell viability compared to POSS-PCU-COOH and control POSS-PCU but not tissue culture plate (TCP) at 3 to 14 days ($p < 0.05$) [D] DNA content significantly increased of the HDFs after 14 days on NH₂ compared to COOH and POSS-PCU from 3 to 14 days ($p < 0.05$). Where, NH₂ is POSS-PCU scaffold modified with allylamine grafting, COOH is POSS-PCU scaffold modified with acrylic acid, and POSS-PCU is Unmodified scaffolds ($n=6$). [E] Protein adsorption was increased after NH₂ and COOH modification compared to unmodified scaffolds at 24 hours ($n=6$) ($p < 0.01$).

127x95mm (300 x 300 DPI)

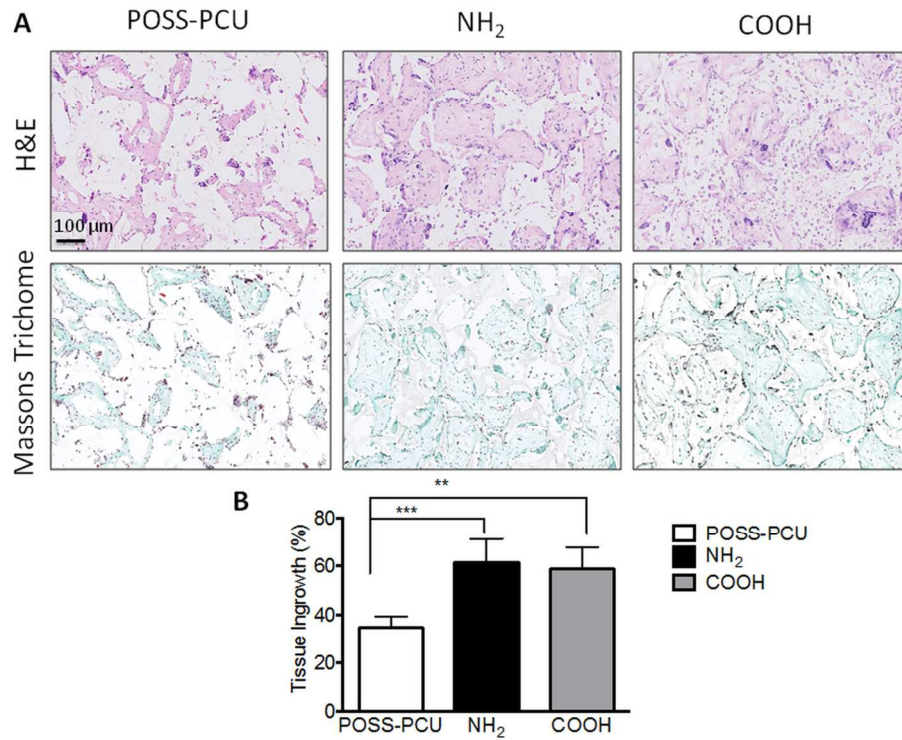


[A] Scanning electron microscopy images of the HDF cells at 14 days, showing cells are laying down a thin extracellular matrix at 14 days on all nanocomposite scaffolds (A-F). [B] Histology using H&E staining taken from the middle of the scaffolds (G-I). Where, NH₂ is POSS-PCU scaffold modified with allylamine grafting, COOH is POSS-PCU scaffold modified with acrylic acid, and control is Unmodified POSS-PCU (n=6).
127x95mm (300 x 300 DPI)



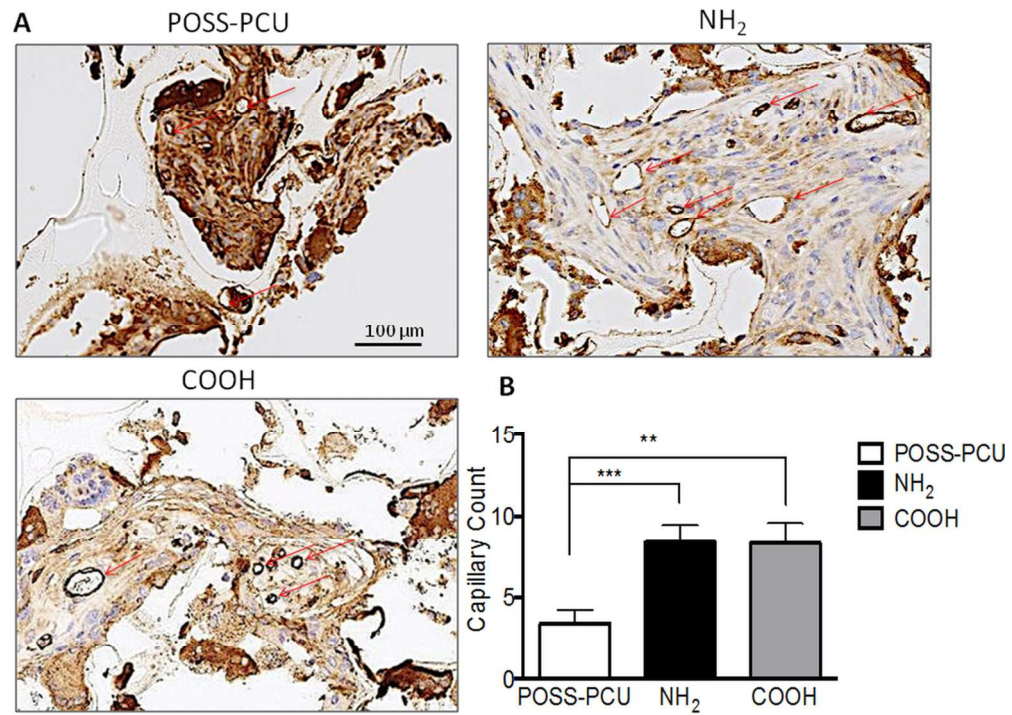
Collagen production produced by human dermal fibroblasts (HDFs) [A] Collagen detected in the supernatant was assessed using Picrosirius Red staining. HDFs seeded on NH₂ showed greater collagen production at 14 days compared to all nanocomposite surfaces including tissue culture plate ($p < 0.05$). [B] Hydroxyproline content was higher by cells seeded on NH₂ and COOH than POSS-PCU ($p < 0.05$). Where, NH₂ is POSS-PCU scaffold modified with allylamine grafting, COOH is POSS-PCU scaffold modified with acrylic acid, and POSS-PCU is Unmodified scaffolds ($n=6$).

127x95mm (300 x 300 DPI)

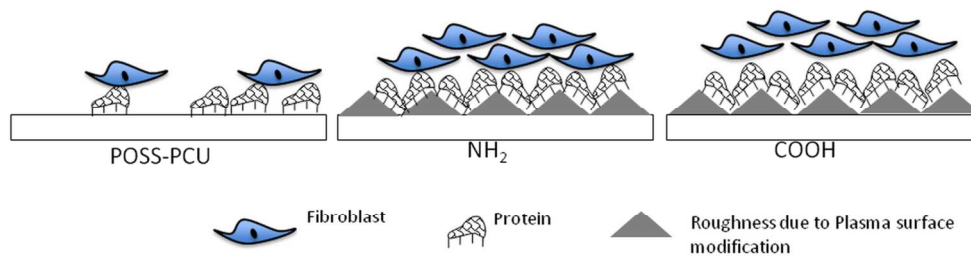


Subcutaneous implantation of POSS-PCU scaffolds after modification with PSM for 12 weeks. [A] Tissue integration assessed by H&E Staining. Collagen production was assessed by Masson Trichome. [B] Quantification of cellular integration and growth after 12 weeks. Where, NH₂ is POSS-PCU scaffold modified with allylamine grafting, COOH is POSS-PCU scaffold modified with acrylic acid, and control is Unmodified POSS-PCU.

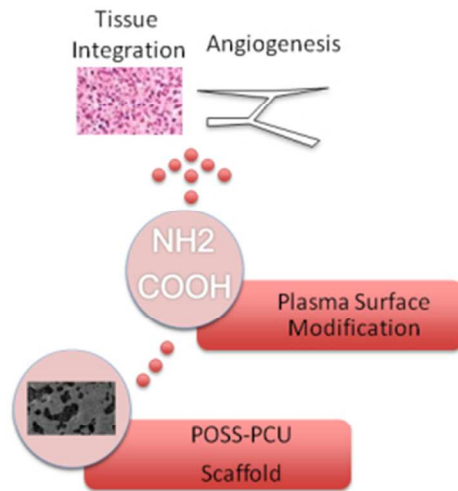
127x95mm (300 x 300 DPI)



[A] Endothelial cell infiltration as identified by CD31 staining, which was used as a marker of angiogenesis.
[B] Quantification of capillary infiltration into the scaffolds after 12 weeks. Where, NH₂ is POSS-PCU scaffold modified with allylamine grafting, COOH is POSS-PCU scaffold modified with acrylic acid, and POSS-PCU is Unmodified scaffolds (n=6).
127x95mm (300 x 300 DPI)



Schematic representation of fibroblast cell attachment to the plasma modified and unmodified scaffolds. The roughness increased on the plasma modified scaffolds, enhance total protein adsorption thus allowing enhance fibroblast attachment of cells at 24 hours.
127x95mm (300 x 300 DPI)



Enhancing tissue integration and angiogenesis of novel nanocomposite polymer using plasma surface modification, an in vitro and in vivo study.
53x39mm (300 x 300 DPI)